Chemical Physics Letters 692 (2018) 271–276

Contents lists available at ScienceDirect

Chemical Physics Letters

journal homepage: www.elsevier.com/locate/cplett

Research paper

REMPI detection of singlet oxygen $^1O_2$ arising from UV-photodissociation of van der Waals complex isoprene-oxygen C_5H_8-O_2

Alexandr S. Bogomolov [a,b], Nikolay V. Dozmorov [a,b], Sergei A. Kochubei [c], Alexey V. Baklanov [a,b,*]

[a] Institute of Chemical Kinetics and Combustion, Novosibirsk, Russia
[b] Novosibirsk State University, Novosibirsk, Russia
[c] Institute of Semiconductor Physics, Novosibirsk, Russia

ARTICLE INFO

Article history:
Received 2 October 2017
In final form 19 December 2017
Available online 20 December 2017

ABSTRACT

The one-laser two-color resonance enhanced multiphoton ionization REMPI [(1 + 1′) + 1] and velocity map imaging have been applied to investigate formation of molecular oxygen in excited singlet $O_2(a^1\Delta_g)$ and ground $O_2(X^3\Sigma_g^-)$ states in the photodissociation of van der Waals complex isoprene-oxygen C_5H_8-O_2. These molecules were found to appear in the different rotational states with translational energy varied from a value as low as ~1 meV to a distribution with temperature of about 940 K. The observed traces of electron recoil in the images of photoions reveal participation of several ionization pathways of the resonantly excited intermediate states of O_2.

1. Introduction

This paper is devoted to the direct REMPI detection of the singlet oxygen arising in the photodissociation of the van der Waals complex of isoprene with oxygen.

Van der Waals (vdW) complex of oxygen X-O_2 is a very suitable model system for the study of the nature of the dramatic influence of the weakly bound environment on the photoinduced processes in oxygen [1–10]. In the cited works the pumping of the electronic excited states of X-O_2 was provided by laser radiation directly [1–8] or by the photodetachment of an electron from the anion X-O_2^- [9,10]. For investigation of the photoprocesses in these complexes the time-of-flight mass-spectrometry [1–3] and velocity map imaging [4–8] as well as photoelectron imaging [9,10] were applied. The results obtained with these weakly bound complexes reveal the dramatic enhancement of O_2 UV-photodissociation yield [1–6] and the appearance of the new channels of O_2 conversion [5–8] as compared with the case of the unbound molecular oxygen. Two of the new channels are assigned to be due to the photogeneration of excited oxygen in the singlet $a^1\Delta_g$ [6–8] and $b^1\Sigma_g^+$ [5] states. Data on the singlet oxygen O_2 formation in photodissociation of vdW complexes X-O_2 are interpreted in terms of double spin-flip (DSF) transition with the simultaneous change of the electronic spin of partner molecules [6–8]

$$^1X - {}^3O_2 + h\nu \rightarrow {}^3X + {}^1O_2 \quad (1)$$

The formation of singlet oxygen was concluded on the basis of the data of velocity map imaging (VMI) of oxygen $O(^3P_j)$ atoms appearing after UV photoexcitation of complexes X-O_2. Among the revealed channels differing by the kinetic energy and the angular anisotropy of the $O(^3P_j)$ atoms' recoil directions there was a channel with the kinetic energy of O atoms equal to about 0.7 eV. This energy corresponds to the kinetic energy of $O(^3P_j)$ atoms arising in the photodissociation of singlet oxygen $O_2(a^1\Delta_g)$ by the same laser pulse via the process

$$O_2(^1\Delta g) + h\nu \rightarrow 2O(^3P_j) \quad (2)$$

This assignment is confirmed by the results recently published by Farook et al. [11] who studied the photodissociation of singlet oxygen with velocity map imaging. In that work singlet oxygen $O_2(^1\Delta_g)$ was generated in a pulsed discharge. The images of the photofragment $O(^3P_j)$ atoms were found to be similar to those observed earlier [5,6] in the photodissociation of complexes X-O_2. In order to test this assignment the direct detection of singlet molecular oxygen is also desirable. The method appropriate for the detection of singlet molecular oxygen in the conditions of molecular beam is the resonance enhanced multiphoton ionization (REMPI). REMPI spectra of singlet oxygen $O_2(^1\Delta_g)$ were obtained by Johnson et al. [12] and Morrill et al. [13]. Johnson et al. generated singlet oxygen with the microwave discharge in O_2. They observed several REMPI bands in the wavelength region 305–350 nm with resolved rotational structure which correspond to the

* Corresponding author at: Institute of Chemical Kinetics and Combustion, Novosibirsk, Russia.
E-mail address: baklanov@kinetics.nsc.ru (A.V. Baklanov).

https://doi.org/10.1016/j.cplett.2017.12.050
0009-2614/

two-photon transitions starting from $O_2(^1\Delta_g, \upsilon'' = 0)$ state. Morrill et al. investigated REMPI (2 + 1) spectra of $O_2(^1\Delta_g)$ with the use of UV-radiation in wavelength region of 310–360 nm [13]. In paper [13] the singlet oxygen $O_2(^1\Delta_g)$ was generated via the photodissociation of ozone. Morrill et al. observed eight bands of $d^1\Pi_g \leftarrow a^1\Delta_g$ transition and provided the detailed characterizations of the rotational structure of the bands corresponding to the transitions into the five lowest vibrational states (v = 0–4) of the $d^1\Pi_g$ state [13].

In the scheme of $O_2(^1\Delta_g)$ REMPI (2 + 1) detection used by Morrill et al. the laser radiation in the wavelength region longer than 300 nm is used. The most investigated system X-O_2 where the photogeneration of $O_2(^1\Delta_g)$ was established is the van der Waals complex of isoprene-oxygen C_5H_8-O_2. The formation of $O_2(^1\Delta_g)$ from this complex was observed in the photoexcitation region 225–260 nm with the maximum of the yield taking place at the shortest wavelengths [6]. So REMPI detection of $O_2(^1\Delta_g)$ arising from complex C_5H_8-O_2 with the use of the (2 + 1) scheme by Morrill et al. [13] can be realized only in a two-laser experiment. But the photoexcitation at a wavelength near 225 nm with REMPI detection of $O_2(^1\Delta_g)$ in a one-laser experiment can be provided with REMPI [(1 + 1′) + 1] scheme used in our recent work detection of the iodine atoms $I(^2P_j)$ [8]. For that we used the radiation of two colors provided by the visible fundamental of pulsed dye laser ($h\nu$) and UV-radiation of its second harmonic ($2h\nu$). This REMPI scheme is shown in Section 3.1 (see Fig. 2). The UV-radiation used in this scheme is applied for the short-wavelength excitation of complex isoprene-oxygen C_5H_8-O_2.

In the current work the results of REMPI and VMI probing of molecular oxygen in singlet and triplet states arising from the UV-photodissociation of van der Waals complex isoprene-oxygen C_5H_8-O_2 are presented.

2. Experimental

The experiments were performed in a vacuum chamber equipped with velocity map imaging setup similar to that one of Eppink and Parker [14]. The van der Waals (vdW) complexes of isoprene with oxygen C_5H_8-O_2 have been generated in a supersonic molecular beam. The beam was created with the home-made electrodynamic pulsed valve mounted in the on-axis configuration by the opening of 0.3 mm nozzle for about 250 μs. In experiments with complexes C_5H_8-O_2 or oxygen itself the valve was filled with a gas mixture of C_5H_8(0.5%) + O_2(5%) + He(balance) or O_2(5%) + He(balance) at a backing pressure 5 bar. After supersonic expansion into the vacuum chamber, the beam was skimmed by a 2 mm skimmer and introduced into the photoexcitation region by passing through the 8 mm diameter hole in a repeller electrode. A laser beam crossed the molecular beam at a right angle. The two-color laser beam has been generated as a fundamental of pulsed dye laser (Coumarine 47, spectral range 450–470 nm, FWHM = 0.01 nm, 10 mJ per pulse) and its second harmonic (1 mJ). The dye laser is pumped by the third harmonic of Nd:YAG laser (355 nm, 120 mJ, 7 ns). The dye laser wavelength was measured by a wavelength meter WS-6 (Angstrom Co). Both the fundamental and the second harmonic were focused on the molecular beam with the use of UV-enhanced aluminum coated spherical mirror with a focal length of 30 cm. The ion optics of VMI spectrometer was similar to that described in the paper [8]. Two extra gard electrodes were inserted between the repeller and the extractor for the better homogeneity of the electric field. The laser was focused into the middle between the gard electrodes. In order to provide the detection of O^+ or O_2^+ ions, the detector was gated at a time corresponding to the time of flight of ions with a mass of 16 or 32 amu, respectively.

3. Results and discussion

3.1. REMPI [(1 + 1′) + 1] spectra of oxygen O_2

In Fig. 1a the REMPI spectra of the oxygen arising from the UV-photoexcitation of the van der Waals complex of isoprene with oxygen C_5H_8-O_2 are presented. The signals of both parent O_2^+ and fragment O^+ ions are recorded in the spectral range of the fundamental wavelength λ_{vac} = 454–470 nm. The excitation of the vdW complex C_5H_8-O_2 is provided by the UV radiation (227–235 nm, $h\nu \approx 5.4$ eV) of the second harmonic of the fundamental. According to the earlier data [6] the yield of singlet oxygen in the UV-region scanned in the current work (227–235 nm) changes only by 10–20%. So, the simultaneous use of scanned UV-radiation for the photoexcitation of the complex and the REMPI detection of appearing $^1O_2$ shouldn't affect the recorded REMPI spectrum of photofragments essentially.

The spectral profiles of O_2^+ and O^+ ions are similar and the O^+ signal is higher in amplitude. The analysis of the possible pathways of the O^+ ions formation in the conditions of REMPI (2 + 1) of O_2 with the use of UV radiation at about 225 nm was carried out by Parker and Eppink [15]. The imaging of O^+ ions and photoelectrons allowed these authors to conclude that about one half of O^+ signal is provided by the one-photon dissociation of a vibrationally excited parent ion O_2^+ produced by the photoionization of O_2 [15]. Another half is provided by the one-photon detachment of an electron from highly excited O atoms arising from the three-photon dissociation of O_2 competing with the photoionization. Because both these final transitions giving rise to O^+ ions are non-resonant one-photon processes the REMPI spectra recorded on the mass of O_2^+ and O^+ ions should be similar. As we see for the better resolved right part of the spectra given in Fig. 1a these spectra are really similar in a major part. So we think that for our scheme of excitation the mechanism of O^+ ions generation is similar.

For comparison we have also converted the REMPI (2 + 1) spectrum of $d^1\Pi_g \leftarrow a^1\Delta_g$ (3,4 ← 0) transitions of singlet oxygen from the paper by Morrill et al. [13] into the wavelength region where these transitions should be located for our scheme of REMPI [(1 + 1′) + 1]. These converted spectra are presented in Fig. 1b with blue lines. Experimental spectrum definitely contains the lines in the expected regions of the REMPI [(1 + 1′) + 1] signal of $O_2(^1\Delta_g)$. In the region of λ_{vac} from 467.31 to 467.959 nm the group of lines corresponding to transitions of R and P branches of $d^1\Pi_g \leftarrow a^1\Delta_g$ (3 ← 0) band starting from the levels with J = 12–18 assigned in the paper [13] are located. The features seen as the lines in Fig. 1 can not be assigned to the individual transitions because they overlap positions of several lines in the better resolved spectrum from paper [13]. The REMPI spectrum in the spectral range of $d^1\Pi_g \leftarrow a^1\Delta_g$ (4 ← 0) transition has very intense extension into the red region (longer than 455.9 nm). This extension is explained by the contribution of the REMPI [(1 + 1′) + 1] signal of the molecular oxygen in the ground state $O_2(X^3\Sigma_g^-)$ which appears also after the photodissociation of complex C_5H_8-O_2. Observed spectrum overlaps well with the spectrum of REMPI (2 + 1) for $O_2(X^3\Sigma_g^-)$ shown by green line in Fig. 1b which is taken from paper by Johnson et al. [12] and converted to the spectral region of our two-photon (1 + 1′) excitation scheme.

Coincidence of the spectral regions of REMPI detected with the regions expected for two-photon (1 + 1′) resonances in the excitation of $O_2(^1\Delta_g)$ state confirms the REMPI [(1 + 1′) + 1] scheme presented in Fig. 2.

So we can conclude that we observe the formation of singlet oxygen $O_2(^1\Delta_g)$ via direct REMPI detection. This result confirms earlier made conclusions on the formation of $O_2(^1\Delta_g)$ which were

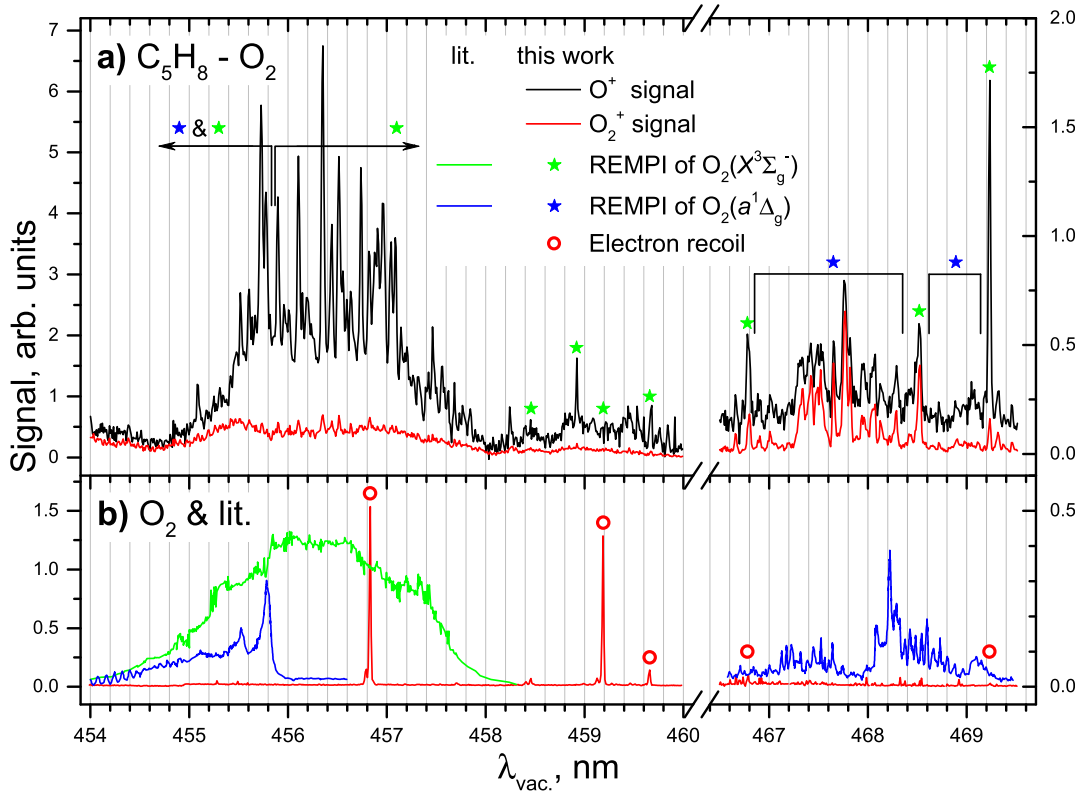

Fig. 1. (a) One-laser two-color REMPI [(1 + 1′) + 1] spectra of oxygen arising from the UV-photoexcitation of the van der Waals complex of isoprene with oxygen C_5H_8-O_2 the spectra are presented as a function of the wavelength of the dye laser fundamental. Blue and green stars mark the lines, stars with arrows or overbraces mark regions, where signals of the singlet $O_2(^1\Delta_g)$ or ground $O_2(X^3\Sigma_g^-)$ state, respectively, are located. (b) Red line – the O_2^+ signal of the ground state of oxygen provided by REMPI of the unbound O_2 in molecular beam (current work). One color REMPI (2 + 1) spectra based on literature data (see text) are also given. Red open circles indicate peaks corresponding to the images with well pronounced effect of electron recoil (see text). (For interpretation of the references to color in this figure legend, the reader is referred to the web version of this article.)

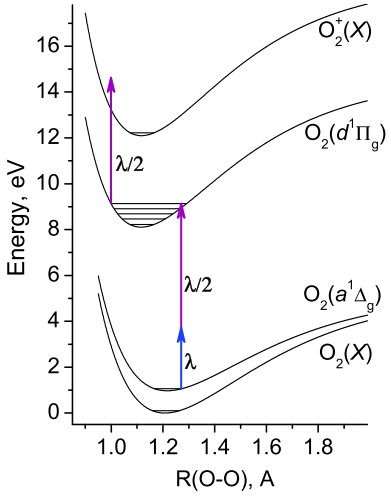

Fig. 2. The scheme of resonance enhanced multiphoton ionization REMPI [(1 + 1′) + 1] of singlet oxygen $O_2(^1\Delta_g)$. Wavelengths λ and λ/2 correspond to the fundamental of dye laser and its second harmonic, respectively.

based on the observation of $O(^3P_j)$ atoms with kinetic energy corresponding to the photodissociation of singlet oxygen $O_2(^1\Delta_g)$ via the process (2) [6–8]. Velocity map image of these $O(^3P_j)$ atoms was found in the cited works to be broad. This broadening was explained with the formation of precursor $O_2(^1\Delta_g)$ molecules to be translationally 'hot' [6]. To verify this we have investigated velocity map images of O_2^+ ions provided by the REMPI [(1 + 1′) + 1] of $O_2(^1\Delta_g)$ discussed in the next section.

In Fig. 1b the REMPI spectrum of only O_2 is also shown which has been obtained by the expansion of O_2 + He mixture. The narrow lines observed belong to the REMPI (2 + 1) of the ground state $O_2(X^3\Sigma_g^-)$ provided by only UV-component of laser radiation (227–235 nm) used in our experiments. These lines exist in the REMPI (2 + 1) spectra of cold O_2 observed by Park et al. [16] and by Yokelson et al. [17] who used tuned UV-radiation corresponding in wavelength to the second harmonic of the fundamental of the dye laser used in our experiments. The comparison of the width of one of these bands (λ_{vac} = 456.83 nm) in the REMPI spectrum of cold O_2 in Fig. 1b with the rotational structure of corresponding REMPI (2 + 1) line available from the paper [16] allows us to conclude that we observe the transitions of Q-branch with low J = 1,3.

3.2. Velocity map imaging of O_2^+ and O^+ ions

Velocity map images (VMI) of O_2^+ ions were measured for all intense lines present in the REMPI spectra shown in Fig. 1. The typical samples of the images are presented in Fig. 3a–c. These images of O_2^+ have no features and look like a blob of different size. Several images contain a bright point in the center like that in Fig. 3a. This bright point corresponds to the ions O_2^+ provided by the REMPI of the translationally cold O_2 molecules.

The observation of translationally cold O_2 in the image allows us to assign corresponding peaks in Fig. 1a marked by green stars to the REMPI lines of $O_2(X^3\Sigma_g^-)$. Here we should indicate that the contribution of the central bright spot into the integral signal of these lines in the REMPI spectrum in Fig. 1a is not large. As it is seen in Fig. 3e the narrow peak with near-zero kinetic energy is

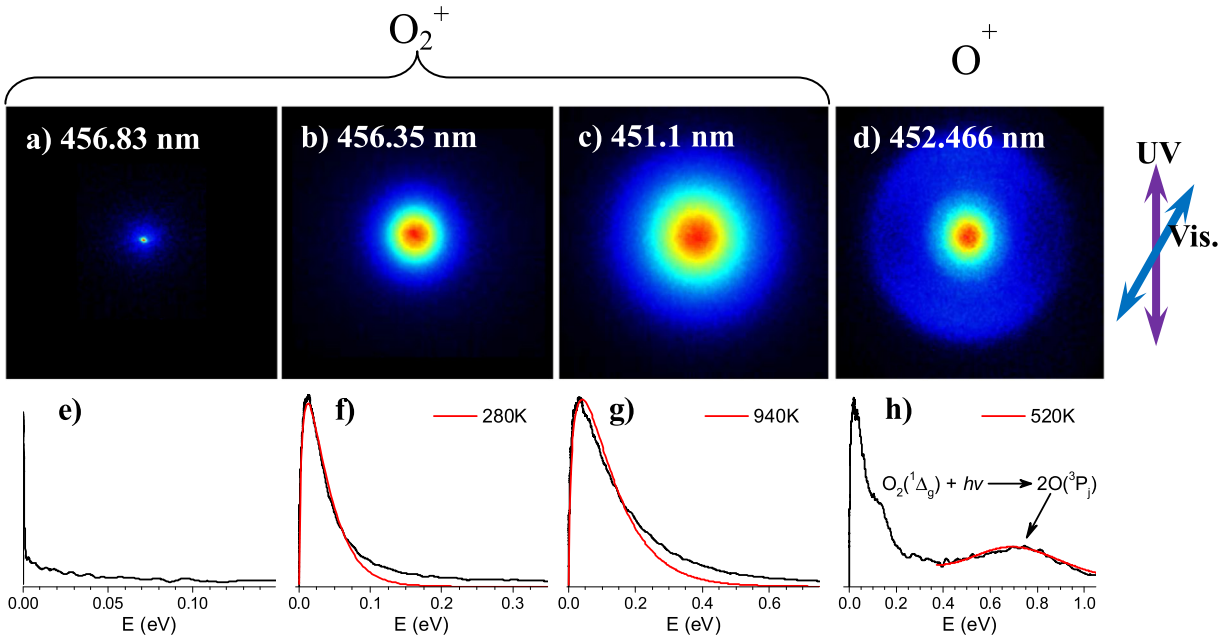

Fig. 3. (a)–(d) Samples of velocity map images of O_2^+ and O^+ ions provided by the photoionization of photofragments arising from C_5H_8-O_2 photodissociation presented numbers correspond to the vacuum wavelength. (e)–(h) Kinetic energy distributions obtained by the Abel inversion of the images presented above red lines correspond to the fit by Maxwell-Boltzmann velocity distribution with the temperature value presented in the figure as well. Double sided arrows indicate the directions of the polarization of Visible (λ) and UV ($\lambda/2$) radiations. (For interpretation of the references to color in this figure legend, the reader is referred to the web version of this article.)

substantially less in integral than the higher energy recoil contributions which is attributed to the translationally 'hot' low-J rotational states of $O_2(X^3\Sigma_g^-)$. In some cases, like at λ_{vac} = 468.516 and 469.234 nm the transitions P(7) and O(14) of the band $d^1\Pi_g \leftarrow a^1\Delta_g$ (3 ← 0) can contribute, respectively.

At the major part of the REMPI lines of both singlet $O_2(^1\Delta_g)$ and triplet $O_2(X^3\Sigma_g^-)$ states the images of O_2^+ ions reveal translationally 'hot' O_2. All these images are isotropic. In Fig. 3b and c two samples of these images are presented. The shapes of corresponding energy distributions obtained by the Abel inversion of these images are shown in Fig. 3f and g. We fitted these profiles with the Maxwell Boltzmann distribution. The profiles obtained by the method of least squares are presented in Fig. 3f and g together with the temperature values corresponding to these fits. The images of O_2^+ provided by REMPI at the other lines have been also fitted in a similar way. Total manifold of the images are characterized by the values of temperature which vary within the range from very low values (see text with the discussion of the image 4e) up to about 940 K. The shape of the images themselves doesn't allow us to discriminate singlet and triplet states.

In Fig. 3d the image of O^+ ions provided by the REMPI (2 + 1) at 226.233 nm of $O(^3P_0)$ atoms arising from the photodissociation of the complex C_5H_8-O_2 at the same wavelength is presented. This image looks similar to that one earlier observed in the paper [6]. The channel assigned to the $O(^3P_0)$ atoms arising from the photodissociation of singlet oxygen in a process (2) gives a broad peak with average kinetic energy near 0.7 eV. This kinetic energy corresponds to atoms provided by the photodissociation of $O_2(^1\Delta_g)$ in the ground vibrational state [6–8]. We have estimated the temperature of the precursor $O_2(^1\Delta_g)$ which fits the observed width of this peak. As it is seen in Fig. 3 h the temperature T = 520 K fits the width very well. Really the peak observed is a result of the convolution of the peaks of $O(^3P_0)$ atoms arising from $O_2(^1\Delta_g)$ molecules in different rotational states with varied kinetic energy distribution which provide the resulted broadened image.

The state distribution of appearing singlet oxygen is governed by the nature of the photoprocess giving rise to $O_2(^1\Delta_g)$. According to the results of the recent studies the photoexcitation of the van der Waals complexes of oxygen X-O_2 gives rise to $O_2(^1\Delta_g)$ via the double spin-flip (DSF) transition [6–8]

$$^3(^1X - {}^3O_2) + h\nu \rightarrow {}^3(^3X - {}^1O_2) \rightarrow {}^3X + {}^1O_2 \quad (^1O_2 = O_2(^1\Delta g)) \tag{3}$$

with the simultaneous change of the spin of both partner molecules but without change of the total spin of the complex. The initial configuration of the complex corresponds to the equilibrium geometry of the van der Waals complex of the molecules X (C_5H_8 in our case) and O_2 in their ground electronic states. In the excited state ^{3}X-$^1O_2$, where both molecules X and O_2 are in their excited electronic states, the minimum of the van der Waals potential is expected to be shifted to a longer X–O_2 distance as compared with the ground state. 'Vertical' excitation should thus deliver the complex to the repulsive branch of the potential in the excited state. This repulsion is responsible for the kinetic energy of appearing $^1O_2$ molecules. In favor of this effect we can refer to our previous paper [18], where analysis of the kinetic energy and the angular distribution of the recoil directions for O atoms arising from photodissociation of X-O_2 complexes was carried out. The released translational energy of the recoil along X-O_2 line, designated as $T_{\|}$, was concluded to effect essentially on the value of experimentally observed angular anisotropy parameter β for the recoil directions of O atoms [18].

Difference in translational temperature of appearing $^1O_2$ molecules can be explained by difference in the initial geometry of the complex X-O_2. Detailed quantum-chemical investigations of the structure have been carried out for the complex of the simplest olefin ethylene with oxygen in papers by DeBoer et al. [2] and by Bogdanchikov and Baklanov [19]. The full optimization carried out in paper [19] showed that two structures correspond to the minima of potential energy. The most stable configuration has the plane structure of C_{2v} symmetry with O_2 molecule directed parallel to the main axis of C_2H_4 molecule. Less stable structure

has C_s symmetry and corresponds to location of O_2 in the plane perpendicular to the main axis of C_2H_4 molecule. In isoprene molecule there are two non-equivalent double C=C and three C—C bonds. So we can expect that the potential energy surface of the van der Waals complex of isoprene with oxygen C_5H_8-O_2 has many local minima corresponding to the different sites of O_2 location near bulky non-symmetrical isoprene molecule. These different sites correspond to the geometries of the complex which differ by the X-O_2 distance and by the relative orientation of the molecules. The 'vertical' excitation in these different configurations delivers the complex to the different positions on the repulsive branch of the potential in the excited state and so gives rise to $^1O_2$ with different kinetic energy. Difference in the distance and the orientation of O_2 relative to C_5H_8 in these different configurations should provide different torques applied to $O_2(^1\Delta_g)$ in the excited state of the complex that results in a variety of rotational states populated by appearing singlet oxygen.

The formation of translationally 'hot' ground electronic state oxygen $O_2(X^3\Sigma_g^-)$ in different rotational states is supposed to be governed by the excitation of isoprene in the complex C_5H_8-O_2

$$^1X - {}^3O_2 + h\nu \rightarrow {}^1X^* - {}^3O_2 \rightarrow {}^1X^* + {}^3O_2 \quad ({}^3O_2 = O_2(X^3\Sigma_g^-)) \qquad (4)$$

Isoprene itself has strong absorption in UV region [20]. The system of π-electrons in isoprene is analogous to that in butadiene. Strong UV-absorption in butadiene is provided by allowed $\pi \rightarrow \pi^*$ transition [21]. Again, in the excited state $^1X^*$–$^3O_2$ the minimum of the van der Waals potential is expected to be shifted to a longer X–O_2 distance as compared with the ground state. So the 'vertical' excitation delivers the complex to the repulsive branch of the potential in the excited state. This repulsion is responsible for the kinetic energy of appearing $^3O_2$ molecules. We can not exclude that the collisions with the fragments of excited isoprene $^1X^*$ dissociation can also contribute to O_2 translational and rotational excitation. We have not found any data about UV-photodissociation pathways in gas phase isoprene. But the energy of photon at the wavelengths used (227–235 nm, $h\nu \approx 5.4$ eV ≈ 124 kcal/mol) is sufficient for the dissociation of isoprene molecule CH_2=C(CH_3)—CH=CH_2 via any of C—H as well as C—CH_3 bonds.

3.3. Ionization pathways in REMPI of $O_2(X^3\Sigma_g^-)$

In Fig. 4a–e the expanded central part of the images of O_2^+ ions are shown. The image which is seen as a point in Fig. 3a looks after expansion in Fig. 4b as the spot with the hole. The expanded images of the ions of cold bare O_2 molecules shown in Fig. 4b–d have holes. These holes are attributed to the effect of electron recoil. The recoil energy is provided by the splitting of translational energy released in the photoionization event. According to the momentum conservation this excess energy is split between O_2^+ ion with m = 32 amu and electron in the proportion of ~1:60,000. We can see this effect of small recoil energy at a level of 0.1 meV for the photoionization of free O_2 molecules in molecular beam because cold O_2 molecules have rather low transversal temperature of about several K (kT ~ 0.25 meV at 3 K). The different sizes

of the holes correspond to recoil from electrons with different kinetic energy provided by the photoionization. Estimates of these recoil energy are presented in Fig. 4 as well. All corresponding REMPI lines were observed by Park et al. and assigned to REMPI (2 + 1) provided by UV radiation [16]. Taking into account that all the intermediate states excited at these lines have very similar energy we conclude that the difference in the recoil energy (presented in the Fig. 4) is governed by the difference in ionization pathways of the intermediate states. For REMPI lines corresponding to images 4b–d the energy of photoelectrons provided by photoionization was measured by Park et al. [16]. According to those data the maximum contribution should be provided by photoelectrons with energy of about 4 eV. But the hole size of only one image presented in Fig. 4d corresponds to this energy. This process just corresponds to REMPI (2 + 1) process (4). Image in Fig. 4a can be assigned to the photoionization of two-UV-photon excited intermediate state by visible photon at 458.92 nm with total REMPI (2 + 1′) process (5). It is worth mentioning that in the experiments by Park et al. [16] this visible radiation also could participate in the photoionization of corresponding intermediate state because these authors didn't filter UV-radiation of the second harmonic from the fundamental radiation used. The biggest hole in the image in Fig. 4b is assigned to the two-UV-photon ionization of the intermediate state with total REMPI (2 + 2) process (6). The hole in Fig. 4c can be provided by two-UV-photon ionization (6) giving rise to ions excited vibrationally or two-(UV + VIS)-photon ionization with total REMPI [2 + (1 + 1′)] process (7). These data definitely indicate the existence of the four-photon processes in the REMPI of the ground state $O_2(X^3\Sigma_g^-)$ in our experimental conditions.

$$O_2(X^3\Sigma_g^-) \overset{2h\nu(UV)}{\rightarrow} O_2^*(Ry) \overset{h\nu(UV)}{\rightarrow} O_2^+ + e \qquad (5)$$

$$\overset{h\nu(VIS)}{\rightarrow} O_2^+ + e \qquad (6)$$

$$\overset{2h\nu(UV)}{\rightarrow} O_2^+ + e \qquad (7)$$

$$\overset{h\nu(UV)+h\nu(VIS)}{\rightarrow} O_2^+ + e \qquad (8)$$

The image 4e shows the ions from slow O_2 molecules with very low kinetic energy at the 1 meV level arising from the complex C_5H_8-O_2. Low kinetic energy of the precursor O_2 molecules allows one to see the holes provided by electron recoil. Two spots are interpreted to be provided by O_2 molecules arising in photodissociation of the complex.

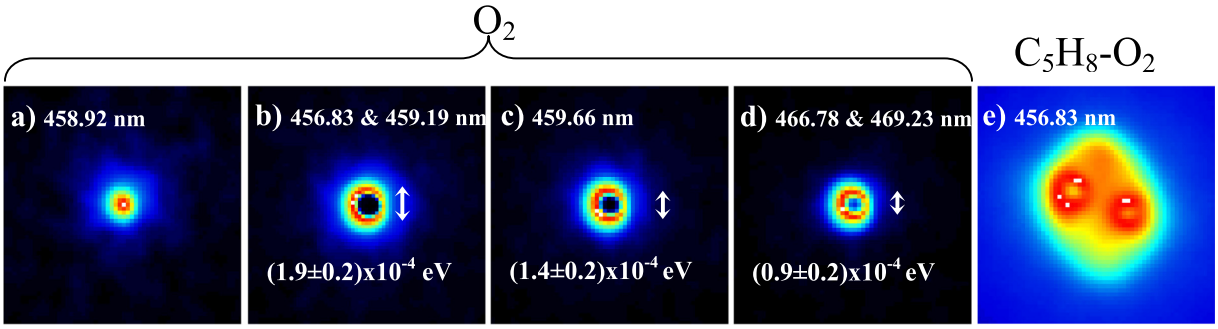

Fig. 4. (a)–(d) Velocity map images of O_2^+ provided by the REMPI of $O_2(X^3\Sigma_g^-)$. The holes in the images correspond to the recoil of photoelectrons detached in the REMPI of O_2 molecules (see text). In figures (b)–(d) the recoil energy extracted from the hole size is presented. e) The image of the very slow $O_2(X^3\Sigma_g^-)$ molecules arising from the photodissociation of complex C_5H_8-O_2. Asymmetry in the location of two rings is attributed to small inhomogeneity in the electric field distribution.

4. Conclusions

The one-laser two-color REMPI [(1 + 1′) + 1] has been applied to detect molecular oxygen O_2 in singlet ($a^1\Delta_g$) and triplet ($X^3\Sigma_g^-$) states arising from the UV-photodissociation of the van der Waals complexes of isoprene with oxygen. The two-photon resonance excitation of O_2 has been provided by the sum of photons of the fundamental of the pulsed dye laser (454–470 nm) and its second harmonic. The spectral regions of REMPI [(1 + 1′) + 1] observed correspond to the earlier measured REMPI (2 + 1) spectra from literature when the energy of resonances was recalculated to the (1 + 1′) excitation scheme. The translational energy of $O_2(a^1\Delta_g)$ and $O_2(X^3\Sigma_g^-)$ was measured with velocity map imaging. Molecules O_2 in both singlet and triplet states were found to appear in different rotational states with translational energy varied from 1 meV level to a distribution corresponding to about 940 K. Measured translational temperature of singlet oxygen allows us to explain the width of the energy distribution of $O(^3P_j)$ atoms arising from singlet oxygen which was observed earlier to appear after the photoexcitation of many van der Waals complexes of oxygen X-O_2. Velocity map images of the O_2^+ cold ions reveal well pronounced effect of the recoil of electrons detached in a REMPI process. Observed values of recoil indicate the contributions of one- and two-photon pathways of the ionization of the resonantly populated intermediate levels.

Acknowledgement

Financial support of this work by the Russian Science Foundation (Grant no 16-13-10024) is gratefully acknowledged. The authors are grateful to Ms Alexandra Svyatova for the help with the treatment of experimental data. The authors thank also the reviewers of the Chemical Physics Letters for very useful recommendations.

References

[1] G. DeBoer, M.A. Young, J. Chem. Phys. 106 (1997) 5468.
[2] G. DeBoer, A. Preszler Prince, M.A. Young, J. Chem. Phys. 115 (2001) 3112.
[3] A. Giardini Guidoni, A. Paladini, M. Veneziani, R. Naaman, T.M. Di Palma, Appl. Surf. Sci. 154 (2000) 186.
[4] B.F. Parsons, D.W. Chandler, J. Phys. Chem. A 107 (2003) 10544.
[5] A.V. Baklanov, G.A. Bogdanchikov, K.V. Vidma, D.A. Chestakov, D.H. Parker, J. Chem. Phys. 126 (2007) 124316.
[6] K.V. Vidma, P.W.J.M. Frederix, D.H. Parker, A.V. Baklanov, J. Chem. Phys. 137 (2012) 054305.
[7] A.V. Baklanov, A.S. Bogomolov, A.P. Pyryaeva, G.A. Bogdanchikov, S.A. Kochubei, Z. Farooq, D.H. Parker, Phys. Chem. Chem. Phys. 17 (2015) 28565.
[8] A.S. Bogomolov, S.A. Kochubei, A.V. Baklanov, Chem. Phys. Lett. 661 (2016) 53.
[9] K.M. Patros, J.E. Mann, C.C. Jarrold, J. Phys. Chem. A 120 (2016) 7828.
[10] K.M. Patros, J.E. Mann, C.C. Jarrold, J. Phys. Chem. A 121 (2017) 5459.
[11] Z. Farook, D.A. Chestakov, B. Yan, G.C. Groenenboom, W.J. van der Zande, D.H. Parker, Phys. Chem. Chem. Phys. 16 (2014) 3305.
[12] R.D. Johnson, G.R. Long, J.W. Hudgens, J. Chem. Phys. 87 (1987) 1977.
[13] J.S. Morrill, M.L. Ginter, E.S. Hwang, T.G. Slanger, R.A. Copeland, B.R. Lewis, S.T. Gibson, J. Mol. Spectrosc. 219 (2003) 200.
[14] A.T.J.B. Eppink, D.H. Parker, Rev. Sci. Instrum. 68 (1997) 3477.
[15] D.H. Parker, A.T.J.B. Eppink, J. Chem. Phys. 107 (1997) 2357.
[16] H. Park, P.J. Miller, W.A. Chupka, S.D. Colson, J. Chem. Phys. 89 (1988) 6676.
[17] R.J. Yokelson, R.J. Lipert, W.A. Chupka, J. Chem. Phys. 97 (1992) 6153.
[18] K.V. Vidma, G.A. Bogdanchikov, A.V. Baklanov, D.A. Chestakov, D.H. Parker, J. Chem. Phys. 133 (2010) 194306.
[19] G.A. Bogdanchikov, A.V. Baklanov, J. Struct. Chem. 56 (2015) 983.
[20] A.P. Pyryaeva, V.G. Goldort, S.A. Kochubei, A.V. Baklanov, Chem. Phys. Lett. 610–611 (2014) 8.
[21] M. Schreiber, M.R. Silva, S.P.A. Sauer, W. Thiel, J. Chem. Phys. 128 (2008) 134110.